

UC Berkeley

UC Berkeley Previously Published Works

Title

Isotopic Evidence for Reductive Immobilization of Uranium Across a Roll-Front Mineral Deposit

Permalink

<https://escholarship.org/uc/item/58x6w8fw>

Journal

Environmental Science and Technology, 50(12)

ISSN

0013-936X

Authors

Brown, Shaun T

Basu, Anirban

Christensen, John N

et al.

Publication Date

2016-06-21

DOI

10.1021/acs.est.6b00626

Peer reviewed

1 Isotopic evidence for reductive immobilization of 2 uranium across a roll-front mineral deposit

3 *Shaun T. Brown*^{1,2*}, *Anirban Basu*^{1,2}, *John N.Christensen*², *Paul Reimus*³, *Jeffrey Heikoop*³,
4 *Ardyth Simmons*³, *Giday Woldegabriel*³, *Kate Maher*⁴, *Karrie Weaver*⁴, *James Clay*⁵ and *Donald*
5 *J. DePaolo*^{1,2}

6 1. Department of Earth and Planetary Science University of California, Berkeley CA USA

7 2. Earth Sciences Division, E.O. Lawrence Berkeley National Laboratory, Berkeley CA USA

8 3. Earth and Environmental Sciences Division, Los Alamos National Laboratory, Los Alamos,
9 NM, USA

10 4. Department of Geological Sciences, Stanford University, Stanford CA USA

11 5. Power Resources Inc., Smith Ranch-Highland Operation 762 Ross Road, Douglas, WY, USA

12
13 Keywords: Uranium isotopes, roll front deposits, natural attenuation

14 15 **Abstract**

16 We use uranium (U) isotope ratios to detect and quantify the extent of natural U reduction in
17 groundwater across a roll front redox gradient. Our study was conducted at the Smith Ranch-
18 Highland *in situ* recovery (ISR) U mine in eastern Wyoming, USA, where economic U deposits
19 occur in the Paleocene Fort Union formation. To evaluate the fate of aqueous U in and adjacent

20 to the ore body, we investigated the chemical composition and isotope ratios of groundwater
21 samples from the roll-front type ore body and surrounding monitoring wells of a previously
22 mined area. The $^{238}\text{U}/^{235}\text{U}$ of groundwater varies by approximately 3‰ and is correlated with U
23 concentrations. Fluid samples down-gradient of the ore zone are the most depleted in ^{238}U and
24 have the lowest U concentrations. Activity ratios of $^{234}\text{U}/^{238}\text{U}$ are ~5.5 up-gradient of the ore
25 zone, ~1.0 in the ore zone, and between 2.3 and 3.7 in the down-gradient monitoring wells.
26 High-precision measurements of $^{234}\text{U}/^{238}\text{U}$ and $^{238}\text{U}/^{235}\text{U}$ allow for development of a conceptual
27 model that evaluates both the migration of U from the ore body and the extent of natural
28 attenuation due to reduction. We find that the pre-mining migration of U down-gradient of the
29 delineated ore body is minimal along eight transects due to reduction in or adjacent to the ore
30 body, whereas two other transects show little or no sign of reduction in the down-gradient
31 region. These results suggest that characterization of U isotopic ratios at the mine planning stage,
32 in conjunction with routine geochemical analyses, can be used to identify where more or less
33 post-mining remediation will be necessary.

34 **Introduction**

35 Nuclear power constitutes approximately 20% of electricity production in the United States
36 and is considered an important component of current energy policy¹. Mining of U ore will
37 continue to be necessary to maintain existing nuclear reactors and support any potential future
38 expansion of nuclear energy. More than 90% of U.S. U production and nearly half of global
39 output comes from *in situ* recovery (ISR) mines². The ISR method improves the economics of
40 mining lower grade ore deposits and potentially reduces the environmental and public health
41 effects relative to traditional underground or open-pit mining techniques. There is little to no

42 surface contamination from radioactive dust, leach ponds or tailings piles because the ore is
43 extracted in an aqueous form.

44 Despite the advantages of ISR mining, there is considerable uncertainty surrounding the
45 restoration of impacted aquifers to pre-mining (baseline) water quality³. A better understanding
46 of the long-term fate of U and other contaminants from ISR mining, particularly fluid-sediment
47 interactions that attenuate U concentrations, would enable industry and regulators to make more
48 informed restoration plans and ensure the integrity of adjacent potable water supplies. For
49 example, geologic formations that host U deposits suitable for ISR mining could have sufficient
50 natural reductive capacity to sequester residual aqueous U after mining and restoration are
51 completed. The reductive precipitation of U is preferred to other sequestration pathways such as
52 sorption, because it is thought to limit U mobility over greater timescales⁴.

53 The reduction of hexavalent U has been widely cited but poorly documented in ISR restoration
54 settings. For example, there is little known about the residual reducing capacity of the sediments
55 and reduction pathways, how the kinetics of reduction reactions compare to groundwater
56 velocities, the effects of aquifer heterogeneity on reduction, or whether the planned duration of
57 groundwater monitoring is sufficient to ensure adequate natural attenuation². The purpose of this
58 study is to highlight how pre-mining distribution of U and its isotopes can provide insights into
59 the removal of U from groundwater. This type of background data and understanding of the
60 natural system is a prerequisite to predicting the fate of U after mining-restoration.

61 The isotopic composition of dissolved U in groundwater is a promising tool for evaluating the
62 fate of U down-gradient of ISR operations. There are two types of isotopic abundance variations:
63 (1) variations in the relative abundance of ²³⁴U in response to natural radioactive decay of ²³⁸U
64 and (2) mass-dependent variations in the ²³⁸U/²³⁵U ratio associated with the chemical reduction of

65 U. Changes in the abundance of ^{234}U , as reflected in the activity ratio of ($^{234}\text{U}/^{238}\text{U}$), arise due to
66 α -recoil of the daughter ^{234}U isotope from mineral grains. The ^{234}U isotope has a recoil distance
67 of 30-40 nm in most silicate minerals and can be either directly ejected from the mineral to
68 groundwater or preferentially leached from radiation induced mineral defects⁵⁻⁷. Large variations
69 of ($^{234}\text{U}/^{238}\text{U}$) in sandstone hosted U deposits have been recognized for more than 50 years but
70 have not been utilized in environmental monitoring or restoration planning at ISR locations^{8,9 10-}
71 ¹².

72 Recent research using environmental samples and laboratory experiments also documents
73 small variations in $^{238}\text{U}/^{235}\text{U}$, a ratio that was long thought to be effectively invariant in most
74 Earth materials¹³. Change of $^{238}\text{U}/^{235}\text{U}$ is primarily associated with reduction of U(VI) to
75 U(IV)^{10,14}, where ^{238}U is preferentially reduced compared to ^{235}U . Experimental and field
76 evidence suggest that the maximum magnitude of instantaneous U isotope fractionation during
77 U(VI)-U(IV) reduction is approximately 1‰ of the $^{238}\text{U}/^{235}\text{U}$ ratio, but residual U that remains
78 after extensive reductive removal can be shifted by several per mil relative to the starting
79 composition^{10-12,14-17}.

80 Prior research on U mobility in fluvial sediments includes the US Department of Energy
81 research sites at Hanford, WA and Rifle, CO¹⁸. At Hanford, the U isotopic compositions of
82 groundwater and pore fluids have been used to trace contamination from nuclear waste storage
83 into the vadose zone and water table, utilizing anthropogenic ^{236}U and variations in $^{238}\text{U}/^{235}\text{U}$
84 from the nuclear fuel cycle in addition to natural variations in ($^{234}\text{U}/^{238}\text{U}$)^{19,20}. In contrast to
85 Hanford, the contamination at the Rifle site involves U with natural isotopic composition.
86 Studies at the Rifle field site include analysis of variations in $^{238}\text{U}/^{235}\text{U}$ during reduction and
87 desorption experiments^{17,21}. These studies find that $^{238}\text{U}/^{235}\text{U}$ is depleted in Rifle groundwater

88 during biostimulation-induced U(VI) reduction and not significantly fractionated by bicarbonate
89 induced desorption. Thus $^{238}\text{U}/^{235}\text{U}$ was found to be a sensitive tracer of U reduction in the Rifle
90 aquifer^{17,21}. Despite the limited natural reduction capacity and high groundwater pore velocities at
91 the Rifle and Hanford sites, these locations are broadly relevant to ISR remediation because they
92 too have artificially elevated U concentrations compared to natural conditions^{20,22} and provide the
93 theoretical framework for research on the fate of aqueous U.

94 More recent work on U isotopes in low-temperature redox-type U deposits includes studies of
95 the ore composition^{11,16,23,24} and studies of groundwater in and adjacent to ore deposits^{12,25-28}. For
96 example, south Texas²⁵ and Australian¹² roll-front ore bodies have decreasing $^{238}\text{U}/^{235}\text{U}$ along the
97 groundwater flow direction that are correlated with decreasing aqueous U concentrations. In the
98 case of South Texas, the ($^{234}\text{U}/^{238}\text{U}$) is generally low in groundwater in contact with the U ore,
99 with higher values up- and down-gradient of the ore body²⁵. The patterns for $^{238}\text{U}/^{235}\text{U}$ and
100 ($^{234}\text{U}/^{238}\text{U}$) are similar for both mined and undeveloped portions of the ore zone. The south Texas
101 and Australian studies identify U reduction as the primary process affecting the $^{238}\text{U}/^{235}\text{U}$ in
102 groundwater and suggest a conceptual isotope fractionation model for interpreting the evolution
103 of the $^{238}\text{U}/^{235}\text{U}$ ratio along the groundwater flow path.

104 Additional isotopic tracers including the short-lived U-series daughter isotopes ^{226}Ra and ^{228}Ra
105 along with the sulfur and oxygen isotopes of sulfate provide additional information about
106 processes influencing U mobility such as reduction and adsorption in the aquifer. Druhan and
107 coworkers^{22,29} used the increasing $\delta^{34}\text{SO}_4$ during biostimulation experiments at the Rifle site to
108 document the onset of microbial sulfate reduction. The $\delta^{34}\text{S}$ of aqueous SO_4 increases as sulfate-
109 reducing microbes utilize the ^{32}S isotope preferentially to the ^{34}S isotope. The isotopes ^{226}Ra and
110 ^{228}Ra are strongly adsorbed to clay minerals in low-TDS, low-chloride groundwater and can be

111 used to measure the sorption capacity of the sediments^{7,30}. The activity ratio of ²²²Rn/²²⁶Ra, for
112 example, can be used to infer the Ra sorption coefficient of the sediments³¹.

113 In this contribution, we present new (²³⁴U/²³⁸U) and ²³⁸U/²³⁵U data for groundwater samples and
114 associated sediments to demonstrate that the isotopic composition of dissolved U in groundwater
115 down-gradient of the ore zone at Smith Ranch, WY is consistent with partial attenuation through
116 reduction of aqueous U. We also demonstrate that ore zone groundwater has distinct U isotopic
117 compositions and that high precision measurements of U isotopes coupled with other
118 geochemical tracers are a sensitive technique for evaluating the extent of U migration and
119 reduction adjacent to an ISR well field.

120 **Hydrogeologic setting**

121 The Smith Ranch-Highland ISR mine is located approximately 50 miles northeast of Casper
122 Wyoming, USA at the southern end of the Powder River Basin (Fig 1 inset). The U ore is
123 concentrated in fluvial sandstones of the Paleocene Fort Union Formation (Fig S1). Regionally
124 the strata dip to the East at <0.5° and groundwater flow is mostly eastward at 2-3 m/yr³².
125 Uranium is concentrated at redox boundaries (roll fronts) that are typically 2-8 meters wide and
126 at depths of 61-366 meters below the surface. Uranium typically occurs as uraninite (UO₂) and
127 coffinite (U(SiO₄)_{0.9}(OH)_{0.4}) coatings on sand grains and is commonly associated with pyrite and
128 carbonaceous matter, which may have facilitated U reduction³³⁻³⁵. The U is thought to have been
129 reduced from the soluble U(VI) to the insoluble U(IV) at a redox interface along the hydraulic
130 gradient, forming crescent-shaped (roll-front) ore deposits.

131 The study area is mining unit 4a (MU4a; Fig 1), which consists of a perimeter ring of
132 monitoring wells and a series of injection and production wells completed within the ore bearing
133 sandstone. The area was mined between 1999 and 2005 using local groundwater fortified with

134 CO₂ and O₂. MU4a entered a restoration phase in 2013, however there were no remediation
135 activities as of our sample collection time except for pumping from recovery wells to maintain
136 negative hydraulic pressure, thus restricting down gradient migration of ore zone fluids. The
137 groundwater analyses have never yielded concentrations of U in excess of the pre-mining values
138 (Fig 1), which implies that the monitor well fluids are not affected by mining.

139 Prior to mining, the monitoring wells in the ore zone and perimeter ring were sampled as part
140 of NRC licensing and characterized for major cations, anions, U, ²²⁶Ra and ²²⁸Ra³². Fluid samples
141 from the wells up-gradient of the ore body had U concentrations of 10-17 ppb. Down gradient
142 samples had concentrations as low as 5 ppb and up to 17 ppb (Fig 1). Aqueous U in the ore zone
143 monitoring wells had 23-72 ppb U with the highest concentrations in the southeast end of the
144 mining unit (Fig 1). The perimeter wells adjacent to the southeastern terminus of the mapped ore
145 body have some of the highest U concentrations and may cross a lower grade portion of the roll
146 front deposit.

147 Baseline wells in the ore zone have ²²⁶Ra activities of 366 to 1625 pCi/L whereas monitoring
148 ring wells have 4.7-35.6 pCi/L down-gradient and 2.9-18.1 pCi/L up-gradient, although up-
149 gradient well M436 has ²²⁶Ra activity of 193.8 pCi/L. The sharp contrast in U and radium
150 concentrations between the ore zone and down-gradient monitoring wells is evidence that prior
151 to mining there was little migration of U or daughter nuclides (such as ²²⁶Ra) down gradient of
152 the ore zone. The mechanisms of radionuclide retention in the ore zone region are not evident
153 from the concentration data alone; however, the apparent sharp gradient in ²²⁶Ra down gradient
154 of the ore body requires processes in addition to reduction because Ra is not a redox sensitive
155 element and the half life of ²²⁶Ra is 1600 years, many times greater than the inferred 50 to 100
156 year transit time of water between the ore zone and the down-gradient monitoring ring. This

157 implies that radium mobility is low, most likely because of adsorption and ion exchange with
158 clays⁷, processes that may also impact U mobility³⁶⁻³⁸. The pre-mining groundwater composition
159 data³⁹ (obtained from NRC website: [http://www.nrc.gov/info-finder/materials/uranium/licensed-](http://www.nrc.gov/info-finder/materials/uranium/licensed-facilities/smith-ranch/isr-wellfield-ground-water-quality-data.html)
160 [facilities/smith-ranch/isr-wellfield-ground-water-quality-data.html](http://www.nrc.gov/info-finder/materials/uranium/licensed-facilities/smith-ranch/isr-wellfield-ground-water-quality-data.html)) summarized above are
161 consistent with a local U mineralized zone surrounded by low U concentration sediments and
162 low U concentration groundwater, an ideal situation for assessing U isotope fractionation
163 associated with a redox boundary and groundwater transport.

164 **Methods**

165 Fluid samples were collected from monitoring wells in MU4a with dedicated down-hole
166 pumps. Wells were purged and then the collected samples were filtered with a 0.45- μm in-line
167 filter and acidified in the case of U isotope aliquots. Samples for S and O isotopes of sulfate were
168 filtered and then aqueous SO_4 was fixed by adding 20% BaCl_2 to precipitate BaSO_4 . Sulfate
169 samples were subsequently acidified with 6M HCl to remove any BaCO_3 .

170 Sediments from the ore zone were recovered from an adjacent mining unit (MU4) by double
171 tube coring and fractions were shipped to Los Alamos National Laboratory³⁵. Sediment aliquots
172 were characterized for mineralogy, elemental composition and isotopic compositions of carbon,
173 U and sulfur³⁵. Separate sediment aliquots were dissolved at UC Berkeley using nitric and
174 hydrofluoric acids and prepared for $\delta^{238}\text{U}$ measurements using the same methods as aqueous
175 samples.

176 Samples for $^{234}\text{U}/^{238}\text{U}$ analysis were purified using Eichrom Tru-Spec resin and analyzed on the
177 GV IsoProbe at Lawrence Berkeley National Laboratory following well-established techniques²⁰.
178 The $^{234}\text{U}/^{238}\text{U}$ ratio is usually discussed in terms of activity (A), where $A=n\lambda$ and n is the number
179 of atoms and λ is the isotope decay constant. In a closed system, the activity of parent and

180 daughter isotopes will reach secular equilibrium ($A_{238U}=A_{234U}$). Thus, variations in $^{234}U/^{238}U$ are
181 described by the activity ratio, [*i.e.*, ($^{234}U/^{238}U$)], where the parentheses denote activity ratio], of
182 the sample compared to secular equilibrium: $(^{n234}U\lambda_{234}/^{n238}U\lambda_{238})_{\text{sample}}/(^{n234}U\lambda_{234}/^{n238}U\lambda_{238})_{\text{secular}}$
183 $_{\text{equilibrium}}$. Measured $^{234}U/^{238}U$ ratios were corrected for ion counting-Faraday cup gain using a
184 secular equilibrium standard and activity ratios were calculated using $\lambda_{234}=2.826\times 10^{-6}$ and
185 $\lambda_{238}=1.551\times 10^{-10}$. The long-term external reproducibility of $^{234}U/^{238}U$ activity ratios at LBNL is
186 better than $\pm 0.3\%$ (2σ).

187 Aliquots of the water samples that were used for $^{238}U/^{235}U$ analysis were spiked with the IRMM
188 3636a ^{233}U - ^{236}U tracer and purified using Eichrom UTEVA resin. The $^{238}U/^{235}U$ ratios were
189 measured on the Nu Instruments MC-ICPMS at Stanford University and are reported as $\delta^{238}U$
190 relative to CRM145. Typical analyses had ^{238}U ion beams of 1.5×10^{-10} A and $^{238}U/^{235}U\sim 18$ -22. The
191 estimated external reproducibility (2σ) of $\delta^{238}U$ measurements is 0.1-0.15‰ based on 98
192 measurements of CRM145. Details of standard measurements are provided in the SI and by refs
193 25 and 40.

194 Sulfur and oxygen isotopes of SO_4 were measured using the Micromass Isoprime at UC
195 Berkeley. Barium sulfate samples were mixed with vanadium oxide, loaded in tin capsules and
196 combusted using the elemental analyzer. Sulfur was measured as SO_2 . Oxygen isotopes of sulfate
197 were measured using pyrolysis and carbon monoxide to make SO_2 . Data were normalized to
198 Canyon Diablo Troilite ($\delta^{34}S$) and SMOW ($\delta^{18}O_{SO_4}$).

199 **Results and Discussion**

200 *Groundwater chemistry from 2012-2014 sampling campaign*

201 The groundwater compositions for baseline (ore zone) and monitoring wells are reported in
202 Table S1 and Figs 1 and S3. Our expectation is that the U ore body represents a redox boundary

203 and that the groundwater U concentration, $\delta^{238}\text{U}$ and ($^{234}\text{U}/^{238}\text{U}$) will all be affected by reactions
204 such as reduction in the ore zone region. The up-gradient groundwater samples have moderate U
205 concentrations 11-16 $\mu\text{g/L}$ and high ($^{234}\text{U}/^{238}\text{U}$) due to the combined effects of α - recoil and the
206 weathering of silicate minerals^{6,41-43}. The $\delta^{238}\text{U}$ is depleted compared to most known groundwater
207 and silicate minerals^{10,12,25,44}. The up-gradient groundwater ($^{234}\text{U}/^{238}\text{U}$) and $\delta^{238}\text{U}$ are tightly
208 clustered varying from 5.12 to 5.61 and -0.88‰ to -1.08‰ respectively, with no discernable
209 correlation with U concentrations.

210 In contrast to the up-gradient groundwater samples, the down-gradient samples display a large
211 range in U concentrations, ($^{234}\text{U}/^{238}\text{U}$) and $\delta^{238}\text{U}$ (Fig 2). Most of the down-gradient samples have
212 U concentrations $<10 \mu\text{g/L}$, lower $\delta^{238}\text{U}$ (-1.5‰ to -2.8‰) and lower ($^{234}\text{U}/^{238}\text{U}$) (< 3.70)
213 compared to the up-gradient water samples (Fig 2). These observations are consistent with the
214 hypothesis that the ore body represents an important reaction zone along the groundwater flow
215 path. Two down-gradient samples from wells M458 and M452 have elevated $\delta^{238}\text{U}$ and U
216 concentrations similar to the up-gradient samples (Fig 2) and thus lack the reduction signature
217 typical of the other down-gradient wells.

218 Groundwater samples from the ore zone collected after mining have high residual U
219 concentrations (13-40 ppm), have relatively high $\delta^{238}\text{U}$ compared to the up-gradient and down-
220 gradient samples, (-0.41‰ to 0.15‰) and have ($^{234}\text{U}/^{238}\text{U}$) near secular equilibrium (0.97-1.11)
221 (Fig. 2). These data are all consistent with residual oxidized U that came from dissolution of U
222 oxide minerals³⁵. The high U concentrations in the ore zone are likely due to some residual
223 oxidation of U and enhanced U(VI) stability in the presence of high bicarbonate concentrations
224 after the completion of mining, at least adjacent to the borehole.

225 Additional inferences about the reducing conditions of the aquifer surrounding the ore zone
226 can be derived from the concentrations of aqueous Fe and SO₄. Fe(III) is largely insoluble, while
227 Fe(II) is soluble in circumneutral pH groundwater, which implies that there should be increasing
228 aqueous Fe concentrations in more reducing groundwater. Aqueous SO₄ concentrations, in
229 contrast, tend to decrease in more reducing groundwater as SO₄ is reduced to HS⁻ and H₂S. The
230 isotope ratios of S and O in aqueous SO₄ increase in response to microbial SO₄ reduction^{22,45}.
231 Concentrations of aqueous Fe for MU4a are generally <100 μg/L in the up-gradient wells and
232 >150 μg/L in the down-gradient wells, consistent with aquifer conditions being sufficiently
233 reducing to cause Fe reduction across the ore body (Fig S2). In the monitoring ring, SO₄
234 concentrations vary between 68 and 157 mg/L while the ore zone well MP423, where there has
235 been induced oxidation, has 896 mg/L SO₄. The ore zone well MP423 is the most depleted in
236 δ³⁴S (-14.1‰), likely due to sulfide mineral dissolution during mining, while the down-gradient
237 wells are generally enriched in δ³⁴S compared to the up-gradient wells (Table 1). The sulfur
238 isotopes indicate that aquifer conditions are sufficiently reducing to cause some sulfate
239 reduction. However, the distribution of δ¹⁸O_{SO4} is less systematic compared to δ³⁴S, with both the
240 most depleted and enriched values found on the down-gradient side of the ore zone. Overall, the
241 variability in δ³⁴S is fairly small compared to roll-front deposits in Texas, where >30‰ of
242 variability is observed in both the fluid and solid phases^{46, 25}. Therefore we conclude that the
243 relatively small variations in δ³⁴S of SO₄ suggest that the aquifer redox potential is just below the
244 threshold for sulfate reduction and not sufficient for widespread or quantitative SO₄ reduction.

245 *Core samples*

246 Characterization of the ore body sediments provides information on the mineralogy and
247 isotopic composition of the reactants in the redox reactions. The U concentrations and activity

248 ratios for core samples collected in previously mined sediments were reported by WoldeGabriel
249 et al³⁵. The sediments have U concentrations from 3 to 25,000 µg/g U and the (²³⁴U/²³⁸U) varies
250 systematically with depth between 1.5 near the top of the ore zone and 0.65 near the bottom of
251 the ore zone. The ore-zone area from 235-238 m (769 to 779 ft) has nearly constant (²³⁴U/²³⁸U) of
252 *ca.* 1.2 and this area also has the highest post-mining U concentrations (1000 to 25,000 µg/g).
253 Three samples from the high U zone were analyzed for δ²³⁸U and are reported in Table 1. The
254 sediment samples range in δ²³⁸U from -0.42‰ to -0.76‰ and are negatively correlated with U
255 concentrations. The δ²³⁸U in the ore samples is intermediate between the up-gradient
256 groundwater and the ore-zone groundwater (Table 1; Fig 2).

257 *Chemical and isotopic evidence for U reduction*

258 Recent research in sandstone hosted U ores and laboratory experiments suggest that ²³⁸U is
259 removed from solution preferentially compared to ²³⁵U during partial reduction of U(VI) to
260 U(IV) into minerals such as uraninite and coffinite^{12,15,47}. The preferential reduction of ²³⁸U(VI)
261 results in decreasing ²³⁸U/²³⁵U in the fluid phase. The reduced and precipitated U(IV) has
262 ²³⁸U/²³⁵U that is determined by the fluid composition and the fractionation factor α :

$$\alpha \equiv \frac{R_p}{R_r} \quad \text{Eq 1}$$

263
264 where R_p and R_r are the ²³⁸U/²³⁵U of the product and reactant respectively. With continued
265 reductive precipitation the fluid U isotope composition should evolve according to a simple
266 (Rayleigh) distillation model^{48,49}:

$$R_{fluid} = R_{initial} \times f^{(\alpha-1)} \quad \text{Eq 2}$$

267
268 Where R_{fluid} is the measured isotopic ratio in groundwater, $R_{initial}$ is the isotopic ratio of the

269 starting groundwater before reductive U removal, f is the concentration expressed as a fraction of
270 the initial U(VI) reservoir and α is the fractionation factor defined above. According to the
271 distillation model when $\alpha > 1$ and U is removed from solution, the $^{238}\text{U}/^{235}\text{U}$ and remaining U
272 concentrations decrease. Though it is difficult to sample the initial dissolved U in natural
273 systems, the quantity of interest is commonly α , which can be calculated by least squares fitting
274 of the measured concentrations and isotopic ratios⁴⁸.

275 A distillation model for the isotopic evolution of the MU4a groundwater was calculated using
276 a least squares regression model of the up-gradient and down-gradient values of $\delta^{238}\text{U}$ and U
277 concentrations. The $\delta^{238}\text{U}$ values of the up-gradient waters are related to the fractionated down-
278 gradient waters by $\alpha = 1.00078(\pm 0.00012)$ when all monitoring well data is considered and
279 $\alpha = 1.00103(\pm 0.00010)$ when only MU4a monitoring wells are considered (Fig. 2; excluded
280 wells are labeled as adjacent in Table S1). The apparent fractionation factor is likely a minimum
281 value as fluid transport effects such as localized reduction, dispersion, and diffusive limitations
282 tend to lessen the observed isotopic fraction compared to the intrinsic fractionation (i.e. observed
283 in laboratory experiments or from theory)^{50,51}. The difference between the MU4a-only and all
284 monitoring well $\delta^{238}\text{U}$ fractionation factors might arise from hydrology effects as the study area
285 size is increased. We discuss this concept in more detail below. Additionally, because sorption
286 does not strongly fractionate U isotopes, U removal by this process will also result in apparent
287 fractionation factors shifted toward unity^{21,52}. The correlated [U] and $\delta^{238}\text{U}$ in MU4a groundwater
288 suggests that U is removed by the reductive precipitation of U(VI) to U(IV).

289 The calculated U isotope fractionation factor is similar to equilibrium fractionation factors of
290 1.00095-1.0013, determined from *ab initio* calculations⁵³ and experiments^{54,55}. Similarly,
291 microbial U reduction experiments have fractionation factors of $\alpha = 1.00068-1.00099$ ^{47,56,57}.

292 Although the exact mechanism of fractionation of U isotopes during irreversible, kinetically
293 controlled aqueous U(VI) reduction is not fully understood, fractionation in the Smith Ranch
294 groundwater is similar in magnitude to both microbial reduction experiments and theoretical
295 predictions of equilibrium inorganic reduction.

296 Other recent studies of roll front deposits have reported smaller fractionation factors of
297 $\alpha=1.00048$ for a south Texas deposit²⁵, and $\alpha=1.00025-1.00054$ for deposits in South Australia
298 (recalculated from published data for each aquifer¹²). The difference between the Smith Ranch
299 fractionation factor and other roll front deposits might be related to the limited spatial extent of
300 the MU4a study area (one sand unit and less than 4 km² area) compared to multiple sand units
301 and greater geographic area at the South Texas and South Australia locations. Sampling over a
302 more limited area may lessen the effects of hydrogeological dispersion and heterogeneity in the
303 sediment lithology, reductants and isotope composition. Alternatively, the reduction mechanism
304 may differ amongst the different roll front deposits. The Smith Ranch aquifers contain abundant
305 fragments of organic carbon, a potential abiotic reductant³⁵, while the south Texas U deposits are
306 thought to form as a result of H₂S gas incursion from stratigraphically lower hydrocarbon
307 reservoirs^{46,58,59} and the south Australian deposits may be a mixture of these reducing materials¹².

308 Chemically reducing conditions between the ore zone and down-gradient monitoring wells in
309 MU4a are also evident from the concentration and isotopic composition of sulfate. In MU4a the
310 lowest [SO₄] and most enriched $\delta^{34}\text{S}$ occur in the same down-gradient wells as the depleted $\delta^{238}\text{U}$
311 (Table S1). The magnitude of $\delta^{34}\text{S}$ fractionation is less than 2‰, which is small compared to
312 fractionations observed in many locations where bacterial sulfate reduction occurs^{22,45,60}. The
313 relatively small degree of SO₄ isotope fractionation is consistent with the observation that sulfur

314 isotope fractionation factors are much smaller when SO_4 concentrations are ~ 1 mM or lower as
315 in the Smith Ranch samples⁴⁵.

316 *Uranium reduction mechanisms and U isotope fractionation*

317 Recent experimental studies suggest that variations in $\delta^{238}\text{U}$ in low temperature environments
318 arise primarily due to direct enzymatic U reduction by microbes and that $\delta^{238}\text{U}$ is not
319 significantly fractionated during inorganic reduction^{56,57}. These inferences reflect the distinctly
320 different U isotope fractionation observed in inorganic reduction experiments and microbial
321 reduction experiments. The microbial experiments are thought to achieve a quasi-equilibrium
322 condition for U isotopes, explaining the similarity to *ab initio* fractionation estimates with ^{238}U
323 enrichment in the product (reduced) phase. In contrast, inorganic magnetite reduction
324 experiments show ^{235}U enrichment in the product (reduced U(IV)) phase, possibly due to kinetic
325 effects that are related to the absence of exchange between the reduced and oxidized reservoirs⁵⁶.

326 The U isotope variations in the MU4a groundwater can be used to infer possible U reduction
327 mechanisms. The fractionation factor we derive is similar to the *ab initio* value, meaning the data
328 could be interpreted as solely microbial U reduction or that the native mixture of inorganic and
329 microbial reductants produce U isotope fractionation similar to the theoretical calculations and
330 dissimilar from the recent inorganic experimental data. Evidence that redox conditions are
331 favorable for inorganic U reduction occur in the relevant aquifer at Smith Ranch includes
332 aqueous Fe(II) concentrations and observations of reduced U on the surfaces of pyrite grains in
333 sediment cores from an adjacent mining area³⁵. The thermodynamic conditions for U reduction
334 by aqueous Fe(II) are likely based on Fe(II) concentrations >100 ppb in the down-gradient wells
335 (*e.g.*, 454, 455A, 458 and 452; Supporting Information Fig S3). The reduction of U by Fe(II)
336 above $\sim \text{pH } 5.5$ is thermodynamically favorable and thought to be kinetically feasible in the

337 presence of abundant mineral surfaces including Fe sulfides⁶¹⁻⁶⁴. The presence of U reduced on
338 the surfaces of lignite and pyrite in the Powder River Basin sediments suggest multiple possible
339 inorganic reduction mechanisms³⁵. If there is a significant amount of non-fractionating U(VI)
340 removal or an opposite sense of isotopic fractionation (*i.e.* ²³⁵U enrichment in remaining U(VI))
341 as observed in laboratory experiments⁵⁶ we should observe smaller apparent fractionation factors
342 inferred from the fractionation model. The calculated fractionation factor for the Smith Ranch
343 fluids is near the *ab initio* values and greater than calculated fractionation factors for South
344 Texas²⁵ and South Australia¹² roll-front deposits, implying that the bulk U reduction process
345 (microbial plus inorganic) both result in the reduced U having higher ²³⁸U/²³⁵U. The discrepancy
346 in U isotope behavior between the Smith Ranch site and inorganic laboratory experiments may
347 indicate that laboratory experiments have yet to capture the behavior of inorganic U reduction in
348 a natural hydrogeologic setting. Alternately the proportion of inorganic U reduction in the
349 reservoir could be small (<10%) compared to microbial reduction and be consistent with the
350 experimental observations⁵⁶. Further experiments with conditions more closely matched to the
351 aquifer mineralogy and fluid compositions may yield a better understanding of the relative roles
352 for inorganic and microbial U reduction in roll front U deposits.

353 *Insights into the spatial distribution of U reduction from ²³⁴U/²³⁸U_{AR}*

354 Although there is evidence of reducing conditions down-gradient of the ore zone, a key
355 question is if reduction is sufficiently fast so that U concentrations are reduced to regulatory
356 limits within an acceptable distance. The observed changes in (²³⁴U/²³⁸U) can be used to estimate
357 the distance over which U is removed by reductive precipitation processes.
358 The model we use assumes that (²³⁴U/²³⁸U) in groundwater is determined by a balance between
359 alpha-recoil related release of ²³⁴U from U-bearing minerals and dissolution of those minerals⁵⁻

360 ^{7,41,65-70}. The data in Fig 3 show that the down-gradient groundwaters have (²³⁴U/²³⁸U) that is
 361 variable but intermediate between the values in the up-gradient water and the ore
 362 zone. However, the down-gradient waters all have lower U concentrations, suggesting net U
 363 removal. Removal can be the result of adsorption or reductive precipitation, but $\delta^{238}\text{U}$ values
 364 suggest that reductive precipitation is the mechanism. Hence a likely scenario is that the water
 365 leaving the ore zone has high [U] and low (²³⁴U/²³⁸U) like the ore zone fluids, and then acquires
 366 higher (²³⁴U/²³⁸U) as a consequence of alpha recoil effects as it moves down gradient. If we
 367 model this process using parameters that we can derive from the up-gradient waters, we can
 368 arrive at estimates of the lengthscale of reductive removal of U.

369 The equation that describes the change in ²³⁴U/²³⁸U with distance is:

370

$$\frac{d(^{234}\text{U}/^{238}\text{U})}{dx} = \frac{1}{L_{\text{weather}}} [A_s - (^{234}\text{U}/^{238}\text{U})] + \frac{1}{L_{\text{recoil}}} \quad (3)$$

371

372 Where x is the horizontal flow distance, A_s is the (²³⁴U/²³⁸U) of the sediments. L_{weather} and L_{recoil}
 373 are described by equations 4 and 5.

374

$$L_{\text{weather}} = qC_f / (\theta M C_s R_d) \quad (4)$$

$$L_{\text{recoil}} = qC_f / (\theta M C_s \lambda_{234} F_a) \quad (5)$$

375

376 where θ is the volumetric water content, M is the solid mass to groundwater volume ratio, C_f and
 377 C_s are the concentrations of U in the groundwater and the solid respectively, λ_{234} is the decay
 378 constant for ²³⁴U ($2.38 \times 10^6 \text{ yr}^{-1}$)⁷¹, q is the groundwater velocity, R_d is the mineral dissolution
 379 time constant and F_a is the fraction of ²³⁸U decays where the daughter isotope is lost from the
 380 mineral.

381 $L_{weather}$ and L_{recoil} control the steady state isotopic composition with distance, and the ratio of
 382 the U concentrations between the solid and the groundwater control the isotopic gradient and the
 383 rate of approach to isotopic steady state. For groundwater beyond the isotopic equilibration
 384 distance, the primary control on ($^{234}\text{U}/^{238}\text{U}$) is the ratio of $L_{weather}/L_{recoil} \sim \lambda_{234}F_d/R_d$ and for
 385 groundwater less than the isotopic equilibration distance, the ratio of $\theta MC_s/C_f$ is also important.

386 The U isotopic equilibration length scales $L_{weather}$ and L_{recoil} for Smith Ranch are on the order
 387 of 5 and 2 km respectively, meaning that water samples at the monitoring ring have not reached
 388 the steady-state ($^{234}\text{U}/^{238}\text{U}$) We assume that θMC_s is a property of the sediments and, similar to
 389 $\lambda_{234}F_d/R_d$, does not vary systematically over the study area, meaning that variations in ($^{234}\text{U}/^{238}\text{U}$)
 390 at the monitoring ring are related to the flow path distance and the groundwater U concentration
 391 between the ore zone and the monitoring ring.

392

393 The quasi-steady state ($^{234}\text{U}/^{238}\text{U}$) of groundwater can be described in terms of distance along the
 394 flow path⁶⁷:

$$(^{234}\text{U}/^{238}\text{U}) = (^{234}\text{U}/^{238}\text{U})_0 \exp\left(-\frac{x}{L_{weather}}\right) + (A_s + \frac{L_{weather}}{L_{recoil}} [1 - \exp\left(-\frac{x}{L_{weather}}\right)]) \quad (6)$$

395

396 where ($^{234}\text{U}/^{238}\text{U}$), ($^{234}\text{U}/^{238}\text{U}$)₀, and A_s are the ($^{234}\text{U}/^{238}\text{U}$) of the groundwater, initial groundwater
 397 and solid respectively.

398 We evaluate 3 scenarios that could describe U transport in the down-gradient region and
 399 compare the predicted ($^{234}\text{U}/^{238}\text{U}$) to the measured down-gradient water samples. Model 1 (M1)
 400 and model 2 (M2) have persistently high (50 $\mu\text{g/L}$) and low (2.5 $\mu\text{g/L}$) U concentrations from the
 401 ore zone to the down-gradient monitoring wells, respectively (Fig 4). These values approximate
 402 the range of [U] observed in the groundwater prior to mining. Model 3 (M3) has a 30 $\mu\text{g/L}$ U

403 concentration from 0-150 m and then 3 $\mu\text{g/L}$ past 150 m corresponding to an instantaneous
404 precipitation event. Eq 6 is solved separately for both segments of M3. This assumes no mixing
405 with upgradient U occurs down gradient of the ore zone. All other parameters are identical for
406 the 3 models and are reported in the caption of Fig 4. Both M2 and M3 show that a decrease in U
407 concentration down gradient is required to generate ($^{234}\text{U}/^{238}\text{U}$) similar to those observed at the
408 monitoring ring (Fig 4). If U reduction is near quantitative in the pre-mining ore zone then the
409 ($^{234}\text{U}/^{238}\text{U}$) at the monitoring ring will be relatively high (Fig 4). Conversely, if groundwater has
410 high U concentrations as it migrates down gradient, this will result in low ($^{234}\text{U}/^{238}\text{U}$) at the
411 monitoring ring.

412 The model results mean that the ($^{234}\text{U}/^{238}\text{U}$) can be used as a tracer to interpolate the fate of
413 aqueous U between the ore zone wells and the monitoring ring and may be helpful for
414 identifying transects where relatively high aqueous U concentrations have migrated down-
415 gradient of the ore zone. In other words, the ($^{234}\text{U}/^{238}\text{U}$) at the monitoring wells will shift toward
416 the ore zone value (in this case <2.5) if groundwater with relatively high aqueous U
417 concentrations migrates toward the monitoring ring, increasing the effective L_{recoil} and L_{weather}
418 equilibration distances. This effect will be detectable prior to U breakthrough at the monitoring
419 wells.

420 The weathering- α -recoil model can be an effective tool for understanding the long-term fate of
421 U mobility in ISR sites after mining-restoration activities are completed. The mining process
422 imparts a distinct $\delta^{238}\text{U}$ -($^{234}\text{U}/^{238}\text{U}$) signature (Table 1; Fig 2), which is less heterogeneous than
423 the pre-mining ore zone fluids and could be easily traced once the natural site hydrology is
424 restored. Both mixing processes in the ore zone and α -recoil-weathering reactions in the down-
425 gradient region require groundwater-mineral exchange reactions in the ore zone and down-

426 gradient regions. The existence of reactions that both add and remove U from the groundwater in
427 the ore zone-down-gradient regions is additionally supported by the wide range of apparent ages
428 for U ore minerals, which are produced by the decoupling of parent and daughter isotopes during
429 dissolution-precipitation reactions⁷². The validity of this model could be more robustly examined
430 with a series of groundwater wells aligned with the flow path and evaluation of the aqueous
431 (²³⁴U/²³⁸U) prior to mining.

432 *Uranium isotope implications for tracking the fate of aqueous ore zone U after remediation*

433 Reduction of aqueous U on the down-gradient edge of the ore body will occur if there are
434 sufficient reducing agents and will occur over a distance dictated by the kinetics of the reduction
435 reaction relative to the fluid velocity. In natural roll-front deposits, the sharp boundaries between
436 mineralized sediments and reduced, unmineralized sediments is evidence that the kinetics of
437 reduction are relatively fast compared to fluid velocity and not a limiting factor for U reduction.

438 Natural attenuation as a component of ISR remediation strategy requires a demonstration that
439 the aquifer down-gradient of mining operations is capable of reducing U and that the kinetics of
440 reduction are sufficiently rapid that U transport is ideally restricted to within the monitoring well
441 ring. We have demonstrated how $\delta^{238}\text{U}$ can be used to track the reduction of U while the
442 (²³⁴U/²³⁸U), along with information about the host sediment and fluid velocities, can be used to
443 estimate the degree to which U is transported down-gradient of the ore zone. Characterization of
444 the pre-mining (²³⁴U/²³⁸U) in the ore zone groundwater would reduce the uncertainty in the model
445 as the interpretation of (²³⁴U/²³⁸U) data in the down-gradient wells will change somewhat if
446 (²³⁴U/²³⁸U) in the ore zone fluids is appreciably higher or lower (Fig 4). In the case of the MU4a
447 study area, there is evidence for both minimal U transport out of the ore zone and substantial U
448 reduction based on the U isotopic data (Figs. 2-4). Two exceptions may be the M458 and M452

449 wells, where the U appears to be a mixture of up-gradient-ore zone sources with little reduction.
450 This suggests that extra attention to the remediation-restoration work up-gradient of the
451 aforementioned wells may be necessary to mitigate down-gradient U transport compared to the
452 rest of the well field. The ability to estimate the contribution of reduction to the overall U
453 attenuation budget (reduction + adsorption) of the aquifer solids could be incorporated into
454 reactive transport models constructed to predict down-gradient concentrations of U.

455
456 Acknowledgements

457 The University of California, Office of the President through the UC Lab Fees Research
458 Program, provided project funding. Cameco Resources provided access and field support for
459 collecting groundwater and sediment core samples. The comments of 3 anonymous reviewers
460 and Associate Editor Daniel Giammar improved the clarity of the manuscript. The US Dept of
461 Energy provided salary support for DJD and JNC during the study period under Contract No.
462 DE-AC02-05CH11231.

463 Supporting Information

464 Details of the site background, ground- water major ion and trace element concentrations, and
465 isotopic data ($\delta^{238}\text{U}$, ($^{234}\text{U}/^{238}\text{U}$), $\delta^{34}\text{S}$, and $^{87}\text{Sr}/^{86}\text{Sr}$). The Supporting Information is available free
466 of charge on the ACS publications website

467

468

- 469 (1) *ALL-OF-THE-ABOVE ENERGY STRATEGY AS A PATH TO SUSTAINABLE ECONOMIC*
470 *GROWTH*; 2014; pp 1–43.
471 [https://www.whitehouse.gov/sites/default/files/docs/aota_energy_strategy_as_a_](https://www.whitehouse.gov/sites/default/files/docs/aota_energy_strategy_as_a_path_to_sustainable_economic_growth.pdf)
472 [path_to_sustainable_economic_growth.pdf](https://www.whitehouse.gov/sites/default/files/docs/aota_energy_strategy_as_a_path_to_sustainable_economic_growth.pdf)
473 (2) Otton, J. K.; Hall, S. In-situ recovery uranium mining in the United States: Overview
474 of production and remediation issues; 2009.
475 [http://www.iaea.org/inis/collection/NCLCollectionStore/_Public/41/003/410032](http://www.iaea.org/inis/collection/NCLCollectionStore/_Public/41/003/41003200.pdf)
476 [00.pdf](http://www.iaea.org/inis/collection/NCLCollectionStore/_Public/41/003/41003200.pdf)

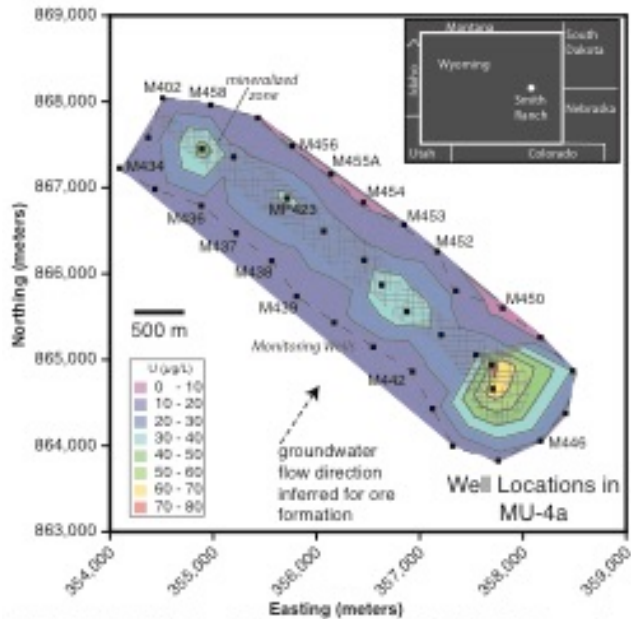
- 477 (3) Hall, Susan. *Groundwater restoration at uranium in-situ recovery mines, South Texas*
478 *coastal plain*. No. 2009-1143. US Geological Survey, **2009**.
- 479 (4) Lovley, D. R.; Phillips, E.; Gorby, Y. A.; Landa, E. R. Microbial reduction of uranium.
480 *Nature* **1991**, 350, 413-416.
- 481 (5) Kigoshi, K. Alpha-Recoil Thorium-234: Dissolution into Water and the Uranium-
482 234/Uranium-238 Disequilibrium in Nature. *Science* **1971**, 173 (3991), 47-48.
- 483 (6) DePaolo, D. J.; Maher, K.; Christensen, J. N.; McManus, J. Sediment transport time
484 measured with U-series isotopes: Results from ODP North Atlantic drift site 984.
485 *Earth Planet. Sci. Lett.* **2006**, 248 (1-2), 394-410.
- 486 (7) Porcelli, D.; Swarzenski, P. W. The Behavior of U- and Th-series Nuclides in
487 Groundwater. *Rev. Mineral. Geochem.* **2003**, 52 (1), 317-361.
- 488 (8) Rosholt, J. N.; Shields, W. R.; Garner, E. L. Isotopic Fractionation of Uranium in
489 Sandstone. *Science* **1963**, 139 (3551), 224-226.
- 490 (9) Rosholt, J. N., E. L. Garner, and W. R. Shields. *Fractionation of uranium isotopes and*
491 *daughter products in weathered granite and uranium-bearing sandstone, Wind River*
492 *Basin region, Wyoming*. National Bureau of Standards, Washington, DC, **1964**.
- 493 (10) Weyer, S.; Anbar, A. D.; Gerdes, A.; Gordon, G. W. Natural fractionation of $^{238}\text{U}/^{235}\text{U}$.
494 *Geochim. Cosmochim. Acta* **2008**, 72, 345-359.
- 495 (11) Bopp, C. J., IV; Lundstrom, C. C.; Johnson, T. M.; Glessner, J. J. G. Variations in
496 $^{238}\text{U}/^{235}\text{U}$ in uranium ore deposits: Isotopic signatures of the U reduction process?
497 *Geology* **2009**, 37 (7), 611-614.
- 498 (12) Murphy, M. J.; Stirling, C. H.; Kaltenbach, A. Fractionation of $^{238}\text{U}/^{235}\text{U}$ by reduction
499 during low temperature uranium mineralisation processes. *Earth Planet. Sci. Lett.*
500 **2014**, 388, 306-317.
- 501 (13) Chen, J. H.; Wasserburg, G. J. Isotopic Determination of Uranium in Picomole and
502 Subpicomole Quantities. *Anal. Chem.* **1981**, 53 (13), 2060-2067.
- 503 (14) Stirling, C. H.; Andersen, M. B.; Potter, E.-K.; Halliday, A. N. Low-temperature
504 isotopic fractionation of uranium. *Earth Planet. Sci. Lett.* **2007**, 264 (1-2), 208-225.
- 505 (15) Brennecka, G. A.; Borg, L. E.; Hutcheon, I. D.; Sharp, M. A.; Anbar, A. D. Natural
506 variations in uranium isotope ratios of uranium ore concentrates: Understanding
507 the $^{238}\text{U}/^{235}\text{U}$ fractionation mechanism. *Earth Planet. Sci. Lett.* **2010**, 291 (1-4),
508 228-233.
- 509 (16) Uvarova, Y. A.; Kyser, T. K.; Geagea, M. L. Variations in the uranium isotopic
510 compositions of uranium ores from different types of uranium deposits. *Geochim.*
511 *Cosmochim. Acta* **2014**, 146 (1-14).
- 512 (17) Charles John Bopp, I. V.; Lundstrom, C. C.; Johnson, T. M.; Sanford, R. A.; Long, P. E.;
513 Williams, K. H. Uranium $^{238}\text{U}/^{235}\text{U}$ Isotope Ratios as Indicators of Reduction: Results
514 from an in situ Biostimulation Experiment at Rifle, Colorado, U.S.A. *Environ. Sci.*
515 *Technol.* **2010**, 44 (15), 5927-5933.
- 516 (18) Maher, K.; Bargar, J. R.; Brown, G. E., Jr. Environmental speciation of actinides. *Inorg.*
517 *Chem.* **2012**, 52, 3510-3532.
- 518 (19) Christensen, J. N.; Dresel, P. E.; Conrad, M. E. Isotopic Tracking of Hanford 300 Area
519 Derived Uranium in the Columbia River. *Environ. Sci. Technol.* **2010**, 44 (23), 8855-
520 8862.

- 521 (20) John N Christensen; P Evan Dresel; Mark E Conrad; Maher, K.; Donald J DePaolo.
522 Identifying the Sources of Subsurface Contamination at the Hanford Site in
523 Washington using High-Precision Uranium Isotopic Measurements. *Environ. Sci.*
524 *Technol.* **2004**, *38* (12), 3330–3337.
- 525 (21) Shiel, A. E.; Laubach, P. G.; Johnson, T. M.; Lundstrom, C. C.; Long, P. E.; Williams, K.
526 H. No Measurable Changes in $^{238}\text{U}/^{235}\text{U}$ due to Desorption–Adsorption of U(VI)
527 from Groundwater at the Rifle, Colorado, Integrated Field Research Challenge Site.
528 *Environ. Sci. Technol.* **2013**, *47* (6), 2535–2541.
- 529 (22) Druhan, J. L.; Conrad, M. E.; Williams, K. H.; N’Guessan, L.; Long, P. E.; Hubbard, S. S.
530 Sulfur Isotopes as Indicators of Amended Bacterial Sulfate Reduction Processes
531 Influencing Field Scale Uranium Bioremediation. *Environ. Sci. Technol.* **2008**, *42*
532 7842–7849.
- 533 (23) Dooley, J. R.; Granger, H. C.; Rosholt, J. N. Uranium-234 fractionation in the
534 sandstone-type uranium deposits of the Ambrosia Lake District, New Mexico. *Econ.*
535 *Geol.* **1966**, *61* (8), 1362–1382.
- 536 (24) Rosholt, J. N., Butler, A. P., Garner, E. L., & Shields, W. R. (1965). Fractionation of
537 uranium isotopes and daughter products in weathered granite and uranium-
538 bearing sandstone, Wind River Basin region, Wyoming. *Econ. Geol. Bull. Soc. Econ.*
539 *Geol.* **1965**, *60*(2), 199–213.
- 540 (25) Basu, A.; Brown, S. T.; Christensen, J. N.; DePaolo, D. J.; Reimus, P. W.; Heikoop, J. M.;
541 WoldeGabriel, G.; Simmons, A. M.; House, B. M.; Hartmann, M.; et al. Isotopic and
542 geochemical tracers for U (VI) reduction and U mobility at an in situ recovery U
543 mine. *Environ. Sci. Technol* **2015**, *49*, 5939–5947.
- 544 (26) Lawson, R. T.; McIntyre, M. G. $^{234}\text{U}/^{238}\text{U}$ signatures associated with uranium ore
545 bodies: part 2 Manyingee. *J. Environ. Radioact.* **2013**, *118*, 157–162.
- 546 (27) Lawson, R. T.; McIntyre, M. G. $^{234}\text{U}/^{238}\text{U}$ signatures associated with uranium ore
547 bodies: part 1 Ranger 3. *J. Environ. Radioact.* **2013**, *118*, 150–156.
- 548 (28) Lawson, R. T. $^{234}\text{U}/^{238}\text{U}$ signatures associated with uranium ore bodies: part 3
549 Koongarra. *J. Environ. Radioact.* **2013**, *118*, 163–168.
- 550 (29) Druhan, J. L.; Steefel, C. I.; Molins, S.; Williams, K. H.; Conrad, M. E.; DePaolo, D. J.
551 Timing the Onset of Sulfate Reduction over Multiple Subsurface Acetate
552 Amendments by Measurement and Modeling of Sulfur Isotope Fractionation.
553 *Environ. Sci. Technol* **2012**, *46* (16), 8895–8902.
- 554 (30) Osmond, J. K.; Cowart, J. B. Ground water. In *Uranium-series disequilibrium:*
555 *applications to earth, marine, and environmental sciences. 2. ed*; 1992.
- 556 (31) Krishnaswami, S.; Graustein, W. C.; Turekian, K. K.; Dowd, J. F. Radium, thorium and
557 radioactive lead isotopes in groundwaters: Application to the in situ determination
558 of adsorption-desorption rate constants and retardation factors. *Water Resour. Res.*
559 **1982**, *18* (6), 1663–1675.
- 560 (32) Smith Ranch Site. [http://www.nrc.gov/info-finder/materials/uranium/licensed-](http://www.nrc.gov/info-finder/materials/uranium/licensed-facilities/smith-ranch.html)
561 [facilities/smith-ranch.html](http://www.nrc.gov/info-finder/materials/uranium/licensed-facilities/smith-ranch.html)
- 562 (33) Dahlkamp, Franz J. Uranium deposits of the world: USA and Latin America. Springer
563 Science & Business Media, 2010.
- 564 (34) *Cameco Resources, License Renewal Application, Technical Report, Table of Contents -*
565 *Chapter 10.0, Part 1 of 4*; 2012; pp 1–302.

- 566 (35) WoldeGabriel, G.; Boukhalfa, H.; Ware, S. D.; Cheshire, M.; Reimus, P. W.; Heikoop, J.;
567 Conradson, S. D.; Batuk, O.; Havrilla, G.; House, B.; et al. Characterization of cores
568 from an in-situ recovery mined uranium deposit in Wyoming: Implications for post-
569 mining restoration. *Chem. Geol.* **2014**, *390*.
- 570 (36) Singer, D. M.; Maher, K.; Brown, G. E., Jr. Uranyl-chlorite sorption/desorption:
571 Evaluation of different U(VI) sequestration processes. *Geochim. Cosmochim. Acta*
572 **2009**, *73* (20), 5989–6007.
- 573 (37) Catalano, J. G.; Brown, G. E., Jr. Uranyl adsorption onto Montmorillonite: Complexity
574 and ongoing challenges. *Geochim. Cosmochim. Acta* **2010**.
- 575 (38) Waite, T. D.; Davis, J. A.; Payne, T. E.; Waychunas, G. A.; Xu, N. Uranium(VI)
576 adsorption to ferrihydrite: Application of a surface complexation model. *Geochim.*
577 *Cosmochim. Acta* **1994**, *58* (24), 5465–5478.
- 578 (39) Smith Ranch Historical Well Field Data. NRC: Washington DC.
579 [http://www.nrc.gov/info-finder/materials/uranium/licensed-facilities/smith-](http://www.nrc.gov/info-finder/materials/uranium/licensed-facilities/smith-ranch/sr-mu-4a.xls)
580 [ranch/sr-mu-4a.xls](http://www.nrc.gov/info-finder/materials/uranium/licensed-facilities/smith-ranch/sr-mu-4a.xls)
- 581 (40) Lau, K. V.; Maher, K.; Altiner, D.; Kelley, B. M.; Kump, L. R.; Lehrmann, D. J.; Silva-
582 Tamayo, J. C.; Weaver, K. L.; Yu, M.; Payne, J. L. Marine anoxia and delayed Earth
583 system recovery after the end-Permian extinction. *Proc. Natl. Acad. Sci. U. S. A.*
584 **2016**, *113* (9), 2360–2365.
- 585 (41) Maher, K.; DePaolo, D. J.; Christensen, J. N. U–Sr isotopic speedometer: fluid flow
586 and chemical weathering rates in aquifers. *Geochim. Cosmochim. Acta* **2006**, *70*
587 (17), 4417–4435.
- 588 (42) Druhan, J. L.; Brown, S. T.; Huber, C. Isotopic Gradients Across Fluid–Mineral
589 Boundaries. *Rev. Mineral. Geochem.* **2015**, *80*, 355–391.
- 590 (43) Maher, K.; DePaolo, D. J.; Lin, J. C.-F. Rates of silicate dissolution in deep-sea
591 sediment: In situ measurement using $^{234}\text{U}/^{238}\text{U}$ of pore fluids. *Geochim. Cosmochim.*
592 *Acta* **2004**, *68* (22), 4629–4648.
- 593 (44) Hiess, J.; Condon, D. J.; McLean, N.; Noble, S. R. $^{238}\text{U}/^{235}\text{U}$ Systematics in Terrestrial
594 Uranium-Bearing Minerals. *Science* **2012**, *335* (6076), 1610–1614.
- 595 (45) Canfield, D. E. Biogeochemistry of Sulfur Isotopes. *Rev. Mineral. Geochem.* **2001**, *43*
596 (1), 607–636.
- 597 (46) Goldhaber, M. B.; Reynolds, R. L.; Rye, R. O. Origin of a South Texas roll-type deposit;
598 II, Sulfide petrology and sulfur isotope studies. *Econ. Geol.* **1978**, *73* (8), 1690–1705.
- 599 (47) Basu, A.; Sanford, R. A.; Johnson, T. M.; Lundstrom, C. C.; Löffler, F. E. Uranium
600 isotopic fractionation factors during U(VI) reduction by bacterial isolates. *Geochim.*
601 *Cosmochim. Acta* **2014**, *136*, 100–113.
- 602 (48) Scott, K. M.; Lu, X.; Cavanaugh, C. M.; Liu, J. S. Optimal methods for estimating kinetic
603 isotope effects from different forms of the Rayleigh distillation equation. *Geochim.*
604 *Cosmochim. Acta* **2004**, *68* (3), 433–442.
- 605 (49) Rayleigh, L. L. Theoretical considerations respecting the separation of gases by
606 diffusion and similar processes. *The London* **1896**.
- 607 (50) Bender, M. L. The $\delta^{18}\text{O}$ of dissolved O_2 in seawater: A unique tracer of circulation
608 and respiration in the deep sea. *J. Geophys. Res.: Solid Earth (1978–2012)* **1990**, *95*
609 (C12), 22243–22252.
- 610 (51) Berna, E. C.; Johnson, T. M.; Makdisi, R. S. Cr stable isotopes as indicators of Cr (VI)
611 reduction in groundwater: a detailed time-series study of a point-source plume.

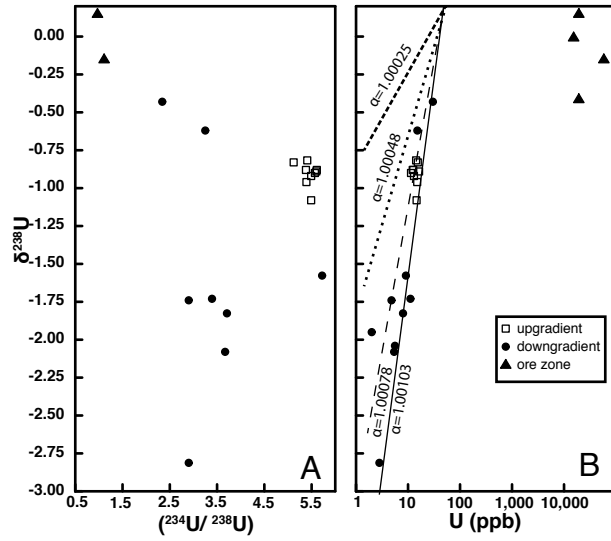
- 612 *Environ. Sci. Technol* **2009**.
- 613 (52) Brennecka, G. A.; Wasylenki, L. E.; Bargar, J. R.; Weyer, S.; Anbar, A. D. Uranium
614 Isotope Fractionation during Adsorption to Mn-Oxyhydroxides. *Environ. Sci.*
615 *Technol* **2011**, *45* (4), 1370–1375.
- 616 (53) Abe, M.; Suzuki, T.; Fujii, Y.; Hada, M.; Hirao, K. An ab initio molecular orbital study
617 of the nuclear volume effects in uranium isotope fractionations. *J. Chem. Phys.* **2008**,
618 *129* (16), 164309.
- 619 (54) Florence, T. M.; Batley, G. E.; Ekstrom, A.; Fardy, J. J. Separation of uranium isotopes
620 by uranium (IV)-uranium (VI) chemical exchange. *J. Inorg. Nucl. Chem* **1975**, *37* (9),
621 1961–1966.
- 622 (55) Fujii, Y.; FUKUDA, J.; KAKIHANA, H. Separation of Uranium Isotopes Using Ion-
623 Exchange Chromatography. *Journal of Nuclear Science and Technology* **1978**, *15*
624 (10), 745–752.
- 625 (56) Stylo, M.; Neubert, N.; Wang, Y.; Monga, N.; Romaniello, S. J.; Weyer, S.; Bernier-
626 Latmani, R. Uranium isotopes fingerprint biotic reduction. *Proc. Natl. Acad. Sci. U. S.*
627 *A.* **2015**, 201421841–201421846.
- 628 (57) Stirling, C. H.; Andersen, M. B.; Warthmann, R. Isotope fractionation of ²³⁸U and ²³⁵U
629 during biologically-mediated uranium reduction. *Geochim. Cosmochim. Acta* **2015**.
- 630 (58) Reynolds, R. L.; Goldhaber, M. B. Iron disulfide minerals and the genesis of roll-type
631 uranium deposits. *Econ. Geol* **1983**, *78* (1), 105–120.
- 632 (59) Goldhaber, M. B.; Reynolds, R. L. Geochemical and mineralogical studies of a south
633 Texas roll front uranium deposit. **1977**.
- 634 (60) Goldhaber, M. B.; Kaplan, I. R. Mechanisms of sulfur incorporation and isotope
635 fractionation during early diagenesis in sediments of the Gulf of California. *Mar.*
636 *Chem.* **1980**.
- 637 (61) Taylor, S. D.; Marcano, M. C.; Rosso, K. M. An experimental and ab initio study on the
638 abiotic reduction of uranyl by ferrous iron. *Geochim. Cosmochim. Acta* **2015**, *156*,
639 154–172.
- 640 (62) Du, X.; Boonchayaanant, B.; Wu, W. M. Reduction of uranium (VI) by soluble iron
641 (II) conforms with thermodynamic predictions. *Environ. Sci. Technol* **2011**, *45* (11),
642 4718–4725.
- 643 (63) Yuan, K.; Renock, D.; Ewing, R. C.; Becker, U. Uranium reduction on magnetite:
644 Probing for pentavalent uranium using electrochemical methods. *Geochim.*
645 *Cosmochim. Acta* **2015**, *156* (C), 194–206.
- 646 (64) Kendall, B.; Komiya, T.; Lyons, T. W.; Bates, S. M.; Gordon, G. W.; Romaniello, S. J.;
647 Jiang, G.; Creaser, R. A.; Xiao, S.; McFadden, K.; et al. Uranium and molybdenum
648 isotope evidence for an episode of widespread ocean oxygenation during the late
649 Ediacaran Period. *Geochim. Cosmochim. Acta* **2015**, *156* (C), 173–193.
- 650 (65) DePaolo, D. J.; Lee, V. E.; Christensen, J. N. Uranium comminution ages: Sediment
651 transport and deposition time scales. *Comptes Rendus ...* **2012**, *344* (11-12), 678–
652 687.
- 653 (66) Lee, V. E.; DePaolo, D. J.; Christensen, J. N. Uranium-series comminution ages of
654 continental sediments: Case study of a Pleistocene alluvial fan. *Earth Planet. Sci.*
655 *Lett.* **2010**, *296* (3-4), 244–254.
- 656 (67) Maher, K.; Ibarra, D. E.; Oster, J. L.; Miller, D. M.; Redwine, J. L.; Reheis, M. C.; Harden,
657 J. W. Uranium isotopes in soils as a proxy for past infiltration and precipitation

- 658 across the western United States. *Am. J. Sci.* **2014**, *314* (4), 821–857.
- 659 (68) Maher, K.; Steefel, C. I.; DePaolo, D. J.; Viani, B. E. The mineral dissolution rate
660 conundrum: Insights from reactive transport modeling of U isotopes and pore fluid
661 chemistry in marine sediments. *Geochim. Cosmochim. Acta* **2006**, *70* (2), 337–363.
- 662 (69) Dosseto, A.; Bourdon, B.; GAILLARDET, J.; Allègre, C. J. Time scale and conditions of
663 weathering under tropical climate: Study of the Amazon basin with U-series.
664 *Geochim. Cosmochim. Acta* **2006**, *70* (1), 71–89.
- 665 (70) Handley, H. K.; Turner, S.; Afonso, J. C.; Dosseto, A. Sediment residence times
666 constrained by uranium-series isotopes: A critical appraisal of the comminution
667 approach. *Geochim. Cosmochim. Acta* **2013**, *103*, 245–262.
- 668 (71) Cheng, H.; Edwards, R. L.; Hoff, J.; Gallup, C. D.; Richards, D. A. The half-lives of
669 uranium-234 and thorium-230. *Chem. Geol.* **2000**, *169* (1-2), 17–33.
- 670 (72) Ludwig, K. R. Uranium-daughter migration and U/Pb isotope apparent ages of
671 uranium ores, Shirley Basin, Wyoming. *Econ. Geol.* **1978**, *73* (1), 29–49.
- 672
- 673
- 674



675
 676 **Fig 1.** Map of the Smith Ranch MU4a well field in eastern Wyoming, USA. Wells in the
 677 perimeter ring are monitoring wells screened in the M sand up and down gradient of the
 678 mineralized sediments. Wells in the center area are baseline wells completed in the M sand
 679 inside the ore body. Contours show the pre-mining distribution of U. Wells in the southeast have
 680 the highest U concentrations while two zones on the presumed down-gradient side of the ore
 681 body are characterized by U concentrations less than 10 ppb (magenta color). Up-gradient wells
 682 are all between 10 and 20 ppb U.

683

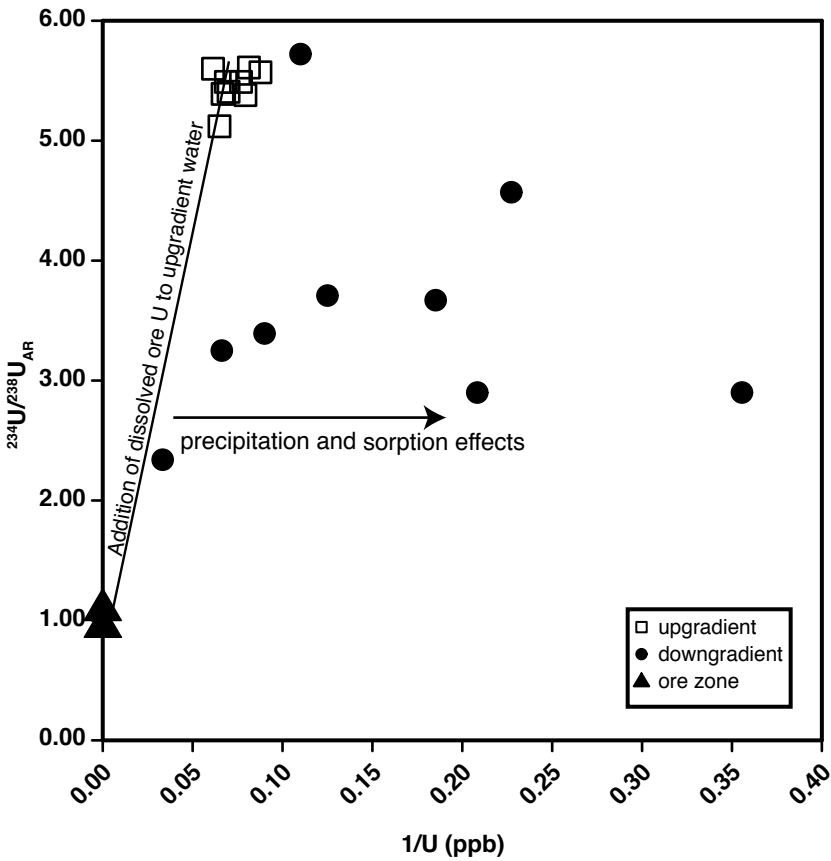


684

685 **Fig 2.** Distribution of U, $^{234}\text{U}/^{238}\text{U}_{\text{AR}}$, and $\delta^{238}\text{U}$ in groundwater in MU4a. Panel B shows the up-
 686 gradient and down-gradient $\delta^{238}\text{U}$ as a function of U concentration. Lines represent distinct
 687 isotopic fractionation factors based on least squares regression of the Smith Ranch data
 688 ($\alpha=1.00078$ and 1.00103), Rosita, TX ($\alpha=1.00048$) and South Australia ($\alpha=1.00025$).

689

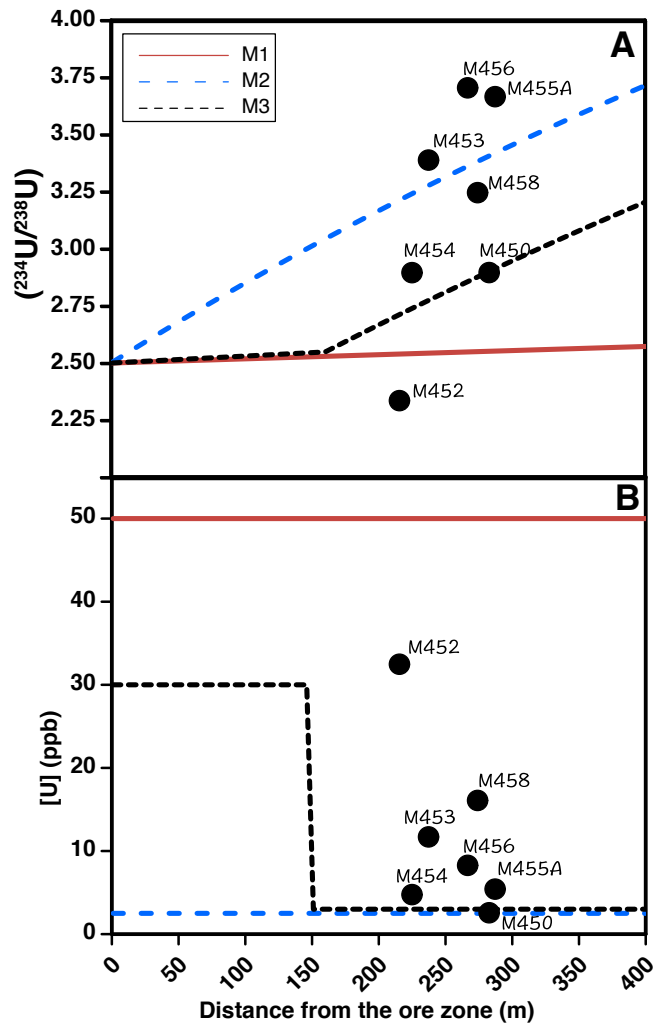
690



691

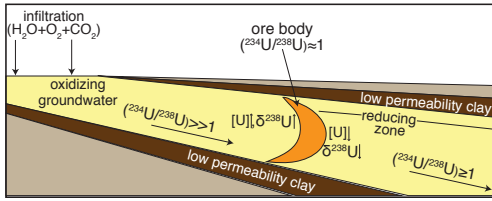
692 **Fig 3.** Mass balance model for the dissolution/desorption of ore zone U to the up-gradient water
693 (legend as in Fig. 2). Notice the down-gradient samples largely fall off the mixing line, requiring
694 sorption/precipitation to lower U concentration between the ore zone and the down-gradient
695 sampling location.

696



697
 698 **Fig 4.** Down-gradient models for $(^{234}\text{U}/^{238}\text{U})$. (A) Models are based on equations presented in the
 699 text. All models use $R_d=8e^{-9} \text{ yr}^{-1}$, $\theta=0.25$, $F_a=0.015$, $C_s=30\text{ppm}$, $q=1 \text{ m/yr}$ and $M_s=25$. M1:
 700 $C_f=50\text{ppb}$, M2: $C_f=2.5 \text{ ppb}$, M3: $C_{f1}=30 \text{ ppb}$ and $C_{f2}=3\text{ppb}$. The strong dependence of the model
 701 curve on C_f demonstrates how down-gradient activity ratios can be affected by water-rock
 702 reaction in the down-gradient region. All model curves have $(^{234}\text{U}/^{238}\text{U})$ equilibration values of
 703 6.5. The diamond symbols are the MU4a down-gradient water samples for reference. (B)
 704 modeled U concentrations for the models presented in panel A and [U] for the down-gradient
 705 groundwater samples. The models M1 and M2 have constant U concentrations, while model M3
 706 has a 90% decrease in aqueous U at 151 m.

TOC ART



707